

# Imaging Somatostatin Positive Tumors with Tyr<sup>3</sup>-Octreotate/Octreotide Conjugated to Desferrioxamine B Squaramide Radiolabeled with either Zirconium-89 or Gallium-68

Asif Noor, Jessica K. Van Zuylekom, Stacey E. Rudd, Peter D. Roselt, Mohammad B. Haskali, Eddie Yan, Michael Wheatcroft, Rodney J. Hicks, Carleen Cullinane, and Paul S. Donnelly\*



Cite This: <https://doi.org/10.1021/acs.bioconjchem.1c00109>



Read Online

ACCESS |



Metrics & More

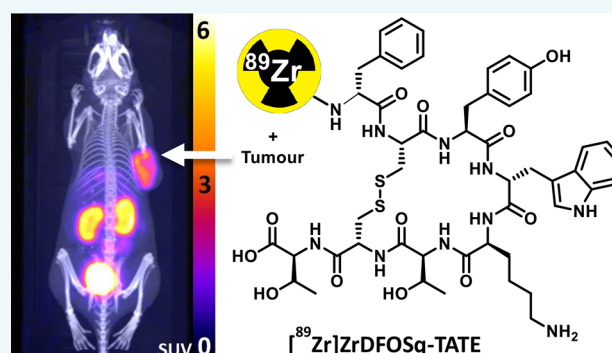


Article Recommendations



Supporting Information

**ABSTRACT:** Radiolabeled derivatives of Tyr<sup>3</sup>-octreotide and Tyr<sup>3</sup>-octreotate, synthetic analogues of the peptide hormone somatostatin, can be used for positron emission tomography (PET) imaging of somatostatin receptor expression in neuroendocrine tumors. In this work, a squaramide ester derivative of desferrioxamine B (H<sub>3</sub>DFOSq) was used to attach either Tyr<sup>3</sup>-octreotide or Tyr<sup>3</sup>-octreotate to the metal binding ligand to give H<sub>3</sub>DFOSq-TIDE and H<sub>3</sub>DFOSq-TATE. These new peptide-H<sub>3</sub>DFOSq conjugates form stable complexes with either of the positron-emitting radionuclides gallium-68 (*t*<sub>1/2</sub> = 68 min) or zirconium-89 (*t*<sub>1/2</sub> = 3.3 days). The new complexes were evaluated in an AR42J xenograft model that has endogenous expression of SSTR2. All four agents displayed good tumor uptake and produced high-quality PET images. For both radionuclides, the complexes formed with H<sub>3</sub>DFOSq-TATE performed better, with higher tumor uptake and retention than the complexes formed with H<sub>3</sub>DFOSq-TIDE. The versatile ligands presented here can be radiolabeled with either gallium-68 or zirconium-89 at room temperature. The long radioactive half-life of zirconium-89 makes distribution of pre-synthesized tracers produced to certified standards feasible and could increase the number of clinical centers that can perform diagnostic PET imaging of neuroendocrine tumors.



## INTRODUCTION

Neuroendocrine cells are regulated by hormones that include somatostatin, a 14-amino-acid peptide, which has a relatively short biological half-life. Neuroendocrine tumors are often characterized by high levels of expression of G-coupled somatostatin receptors (SSTR), especially the somatostatin subtype 2 receptor.<sup>1,2</sup> Synthetic peptide analogues of somatostatin which retain affinity for the receptor but are more metabolically stable are useful agents for both diagnostic imaging and therapy of neuroendocrine tumors. An example is an 8-amino-acid peptide called octreotide (DPhe-c[Cys-Phe-DTrp-Lys-Thr-Cys]-Thr-ol) (Figure 1) radiolabeled with  $\gamma$ -emitting indium-111, [<sup>111</sup>In]In(DTPA-octreotide) (DTPA = diethylenetriaminepentaacetic acid), which is used for diagnostic single photon emission computed tomographic (SPECT) imaging of neuroendocrine tumors.<sup>3</sup> Further refinements in SSTR targeting peptides involved substitution of the third phenylalanine for tyrosine to give [Tyr<sup>3</sup>]-octreotide and by replacing the C-terminal threoninol with threonine to give [Tyr<sup>3</sup>]-octreotate (DPhe-c[Cys-Tyr-DTrp-Lys-Thr-Cys]-Thr) (Figure 1).<sup>4–8</sup> Positron emission tomography (PET) imaging offers superior resolution to SPECT imaging, and this has led to developments that take advantage of the positron-emitting radionuclide gallium-68 and conjugates of the macrocyclic

chelator DOTA (1,4,7,10-tetraazacyclododecane-1,4,7,10-tetraacetic acid).<sup>9</sup> A current approach for the treatment of somatostatin positive tumors is to use diagnostic PET imaging with the gallium-68 complex of DOTA-Tyr<sup>3</sup>-octreotide (DOTATOC) or DOTA-Tyr<sup>3</sup>-octreotate (DOTATATE) to guide peptide receptor radionuclide therapy (PRRT) using therapeutic radionuclides such as the  $\beta$ -emitting lutetium-177 or yttrium-90.<sup>6,10–12</sup>

The rapid growth in diagnostic PET imaging with gallium-68 radiopharmaceuticals has been made possible by relatively easy access to the radionuclide from germanium-68/gallium-68 generators.<sup>13,14</sup> The production of gallium radiopharmaceuticals still requires a dedicated on-site radiopharmacy/radiochemistry team, as the relatively short radioactive half-life of gallium-68 (*t*<sub>1/2</sub> = 68 min) limits the potential for centralized production and distribution. The rapid growth in gallium

**Special Issue:** State-of-the-Art of Radiometal-based Bioconjugates for Molecular Imaging and Radiotherapy

**Received:** March 2, 2021

**Revised:** March 15, 2021

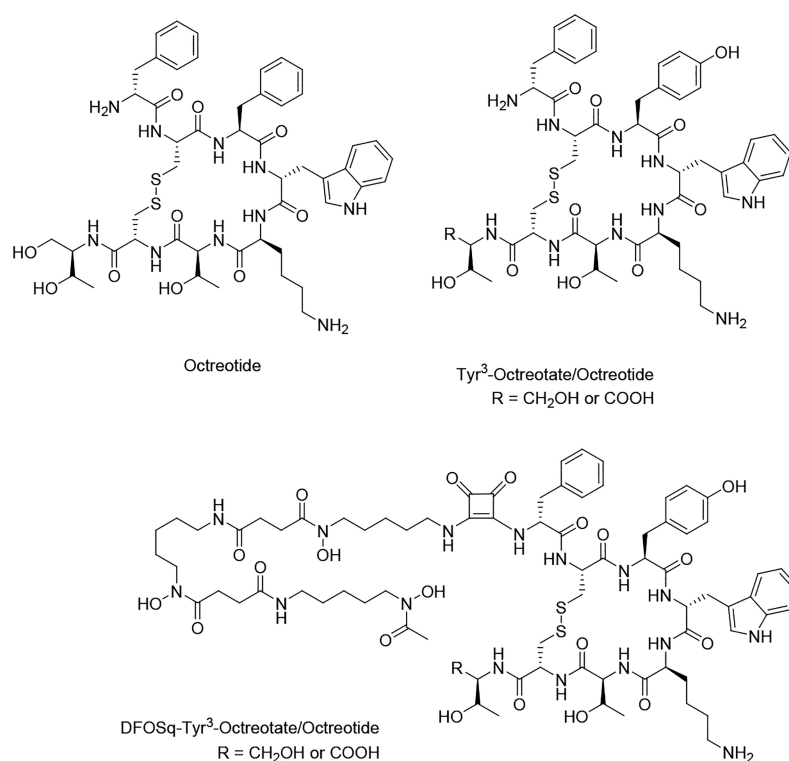


**Figure 1.** Structures of octreotide, Tyr<sup>3</sup>-octreotide, Tyr<sup>3</sup>-octreotate, and DFOSq-TIDE/TATE.

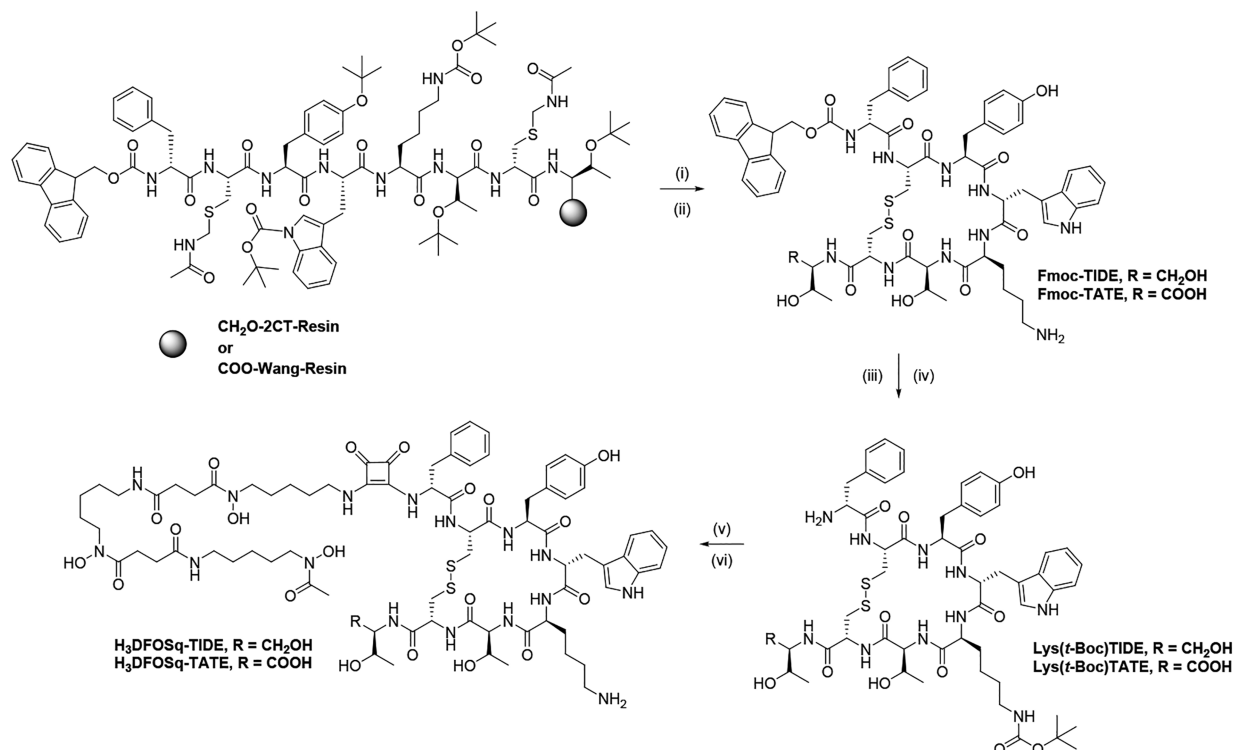
radiopharmaceuticals has led to shortages of germanium-68/gallium-68 generators in some regions. Consequently, SSTR imaging agents that use other positron-emitting radionuclides, including fluorine-18,<sup>15,16</sup> copper-64,<sup>17–20</sup> scandium-44,<sup>21,22</sup> and terbium-152<sup>23</sup> are of interest (for a review of next generation SSTR PET imaging agents, see ref 24). The relatively long radioactive half-life of positron-emitting zirconium-89 ( $t_{1/2} = 3.3$  days) is well suited for manufacturing radiopharmaceuticals to certified standards and then regional distributions from centralized manufacturing sites. The relatively low positron emission translational energy of zirconium-89 (395.5 keV) could offer better resolution than images acquired using gallium-68 that has a higher positron emission translational energy (830 keV).<sup>14,25,26</sup> However, a significant disadvantage of zirconium-89 is that the positron emission leads to the formation of yttrium-89m, which then decays to yttrium-89 through a relatively high-energy  $\gamma$ -emission (920 keV) adding to radiation exposure. Safe transport of zirconium-89 radiopharmaceuticals would require more shielding than what is routinely used for shipping fluorine-18 radiopharmaceuticals.<sup>25</sup>

A single versatile SSTR targeting ligand that could be radiolabeled with either gallium-68 or zirconium-89 could be useful in that the selection of radionuclide could be chosen depending on local availability. The ability to centrally manufacture the zirconium-89 analogue for distribution could improve the feasibility of PET imaging at clinical sites without on-site radiochemistry expertise. In recent work, aimed at preparing receptor targeting ligands that can be radiolabeled with either zirconium-89 or gallium-68, we used a version of the bacterial siderophore, desferrioxamine B (H<sub>3</sub>DFO) that has been modified by the addition of a squaramide ethyl ester functional group to give H<sub>3</sub>DFOSquaramide (H<sub>3</sub>DFOSq) to attach glutamate-ureido-lysine small molecules that target

prostate-specific membrane antigen.<sup>27</sup> The potential of derivatives of H<sub>3</sub>DFO to coordinate gallium-67 and gallium-68 radionuclides has been demonstrated previously.<sup>27–32</sup> For example, a [<sup>67</sup>Ga][Ga(DFO)] complex was demonstrated as being sufficiently stable in human serum for 2 days.<sup>29,33</sup> Zirconium(IV) complexes of the squaramide ester derivative, DFOSqOEt, are more resistant to ligand exchange than zirconium(IV) complexes with DFO derivatives prepared using the isothiocyanate derivative, H<sub>3</sub>DFO-C(S)-NH-PhNCS, and have better solubility in aqueous mixtures.<sup>34,35</sup> The coupling of squaramide ethyl esters to the amino groups of peptides is straightforward and does not involve the use of additional coupling agents. In this work, we extend the approach to attach the cyclic peptides Tyr<sup>3</sup>-octreotate and Tyr<sup>3</sup>-octreotide to DFOSq. The gallium-68 and zirconium-89 complexes of the new conjugates were evaluated in an AR42J xenograft model.

## RESULTS

**Synthesis of H<sub>3</sub>DFOSq-TIDE/TATE.** The resin-bound linear Tyr<sup>3</sup>-octreotide/tate peptides were prepared using standard microwave-assisted automated solid-phase peptide synthesis. Each amino acid coupling involved the use of the respective Fmoc protected amino acids, 1-[bis-(dimethylamino)methylene]-1*H*-1,2,3-triazolo[4,5-*b*]pyridinium 3-oxide hexafluorophosphate (HATU) and diisopropylethylamine (DIPEA) as the base. Deprotection of Fmoc groups was achieved with 20% piperidine in dimethylformamide (DMF) after each cycle, but no final *N*-terminus Fmoc deprotection was performed. Cyclization of the peptides through the formation of an intramolecular disulfide bridge between the second and seventh cysteine residues was achieved by *in situ* deprotection of acetamido methyl (Acm) group on cysteine residues followed by oxidation with iodine in DMF. Conjugation of H<sub>3</sub>DFOSquarate to amino acids

Scheme 1. Synthesis of H<sub>3</sub>DFOSq-TATE/TIDE Peptides<sup>a</sup>

<sup>a</sup>(i) Iodine, DMF; (ii) TFA cocktail; (iii) *t*-Boc-anhydride, DIPEA, DMF; (iv) 20% piperidine in DMF; (v) H<sub>3</sub>DFOSqOEt, 0.1 M borate buffer, pH 9.0, (vi) 20% TFA in DCM.

proceeds well in aqueous borate buffer (0.1 M, pH ~ 9) which is not compatible with the resin used for solid-phase peptide synthesis. Consequently, following cyclization, the peptide was cleaved from the resin and global deprotection of the remaining protecting groups was achieved using a standard trifluoroacetic acid mixture (Scheme 1) prior to conjugation to H<sub>3</sub>DFOSq in solution. To attach a single H<sub>3</sub>DFOSq specifically on *N*-terminus *D*-Phe<sup>1</sup> unit, the side chain amine group of Lys<sup>5</sup> was protected using *t*-Boc anhydride followed by removal of the Fmoc group from the *N*-terminus using 20% piperidine in DMF. The resulting Lys<sup>5</sup>(*t*-Boc)-TATE/TIDE peptides were conjugated to H<sub>3</sub>DFOSq by incubating the mixture in 0.1 M borate buffer (pH ~ 9.0, 10% DMSO) over 7 days. The deprotection of the *t*-Boc group on Lys<sup>5</sup> allowed isolation of H<sub>3</sub>DFOSq-TATE/TIDE peptides in ~25–28% yield (Scheme 1).

**Radiolabeling of H<sub>3</sub>DFOSq-TATE/TIDE with Either Gallium-68 or Zirconium-89.** Radiolabeling of both H<sub>3</sub>DFOSq-TATE and H<sub>3</sub>DFOSq-TIDE with [<sup>68</sup>Ga]Ga<sup>III</sup> was achieved at room temperature in 10 min. The modified peptides were added to aqueous mixtures of [<sup>68</sup>Ga]Ga<sup>III</sup>, obtained from elution of a germanium-68/gallium-68 generator with 0.05 M HCl, following partial neutralization to pH 4–5 with sodium acetate buffer (1 M, pH 4.5). Even with the use of a relatively low peptide mass (approximately 150 ng/MBq of [<sup>68</sup>Ga]Ga<sup>III</sup>), it was possible to obtain [<sup>68</sup>Ga]-GaDFOSq-TATE and [<sup>68</sup>Ga]GaDFOSq-TIDE in high radiochemical yield and purity (≥98%, 150 ng, 0.08 nmol/MBq) requiring no purification for *in vivo* experiments (Figure 2).

The conditions for radiolabeling with zirconium-89 were extrapolated from our previous work with H<sub>3</sub>DFOSq conjugated to lysine-ureido-glutamate.<sup>27</sup> Both peptides were

labeled with zirconium-89 at a concentration of 2 μg/MBq (1.1 nmol/MBq). Analysis by radio-HPLC shows radiochemical yield of >95% in 30 min at room temperature. The crude tracers were then purified by passage through Phenomenex Strata-X C18 cartridges using ethanol as eluent to give the tracers in >98% radiochemical purity (Figure 2).

The resistance of the new complexes to radiolysis was investigated by incubating the purified radiolabeled peptides in phosphate buffered saline at room temperature for 4 h for <sup>68</sup>Ga labeled peptides (18 MBq, 100 μL) or 96 h for zirconium-89 labeled peptides (2.5 MBq, 220 μL). For each peptide, analysis of the samples by radio-HPLC suggests <5% decomposition to more hydrophilic uncharacterized compounds with shorter retention times, presumably due to radiolysis (Figure S11). [<sup>89</sup>Zr]ZrDFOSq-TATE was selected for preliminary investigations with higher amounts of radioactivity (100 MBq) which was labeled with H<sub>3</sub>DFOSq-TATE (2.5 μg) in 15 min at 75 °C to give >98% radiochemical yield. The stability of this preparation (~66 GBq/μmol) in a mixture of PBS, ethanol (10%), and sodium gentisate (0.5%) was monitored by analysis by HPLC. After 5 days, the purity of [<sup>89</sup>Zr]ZrDFOSq-TATE was ~75% with the major decomposition product leading to a peak in the HPLC with a shorter retention time (Figure S13, SI).

**PET-CT Imaging and Biodistribution in SSTR2 Positive AR42J Xenograft Mice Models.** [<sup>68</sup>Ga]-GaDFOSq-TIDE and [<sup>68</sup>Ga]GaDFOSq-TATE tracers were injected (2–3 MBq, 1 μg, 0.5 nmol) intravenously via tail vein to AR42J (rat pancreatic cancer cell line) tumor-bearing Balb/c nude mice. PET images were acquired at 1 and 2 h post-injection (Figure 3a and b). The tumor uptake in the PET images is clear for both tracers, but [<sup>68</sup>Ga]GaDFOSq-TATE

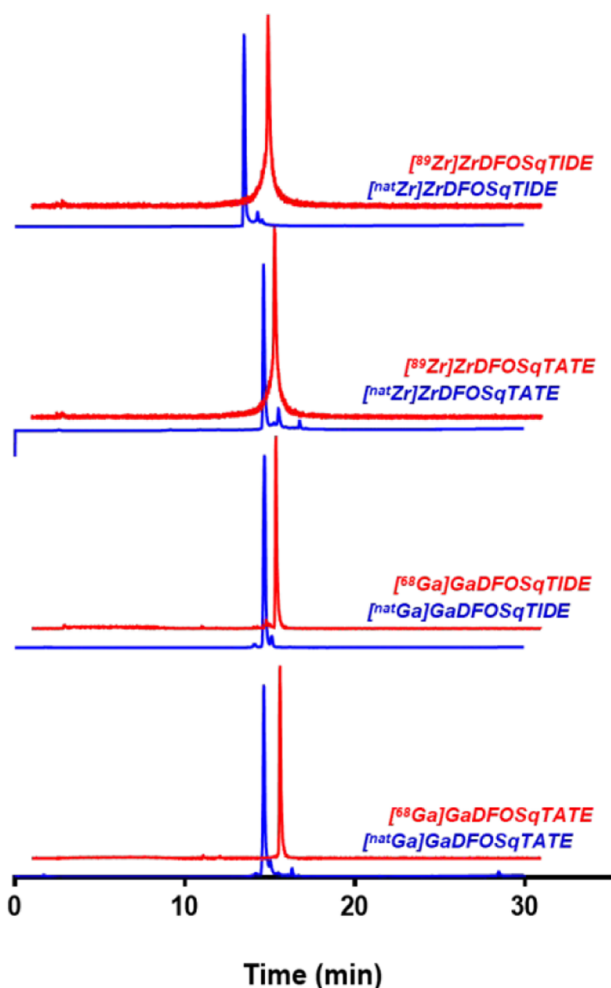


**Figure 2.** Radio-HPLC chromatograms of  $[^{89}\text{Zr}]$ ZrDFOSq-TATE/TIDE and  $[^{68}\text{Ga}]$ GaDFOSq-TATE/TIDE peptides (red, radiation detection) compared against nonradioactive analogues,  $[^{\text{nat}}\text{Zr}]$ -ZrDFOSq-TATE/TIDE and  $[^{\text{nat}}\text{Ga}]$ GaDFOSq-TATE/TIDE (blue,  $\lambda_{\text{abs}} = 254 \text{ nm}$ , offset for clarity, gradient method: 0–100% solvent B to A over 25 min, solvent A = 0.05% TFA in Milli-Q water and solvent B = 0.05% TFA in  $\text{CH}_3\text{CN}$ ).

has higher tumor uptake. Quantification of the uptake in the images using standard uptake value ( $\text{SUV}_{\text{max}} = \text{radioactivity in a tissue (Bq/mL)} \times \text{body weight (g)}/\text{injected activity (Bq)}$ ) confirms the higher uptake for  $[^{68}\text{Ga}]$ GaDFOSq-TATE (1 h;  $\text{SUV}_{\text{max}} = 1.8 \pm 0.2$ , compared to  $1.21 \pm 0.20$ , Figure 3c). The higher tumor uptake of  $[^{68}\text{Ga}]$ GaDFOSq-TATE was also associated with a higher degree of tumor retention at 2 h post-injection with only a 5% reduction in  $\text{SUV}_{\text{max}}$ , whereas the tumor  $\text{SUV}_{\text{max}}$  for  $[^{68}\text{Ga}]$ GaDFOSq-TIDE reduced by 30% at 2 h post-injection. Addition of an excess of the respective nonradioactive peptides (20  $\mu\text{g}$ , 11.1 nmol per mouse) results in a significant reduction in tumor uptake, suggesting the uptake of both tracers in the tumor is receptor mediated (Figure 3).

The high tumor uptake was confirmed by an *ex vivo* biodistribution study in the same mouse model where mice were injected with either  $[^{68}\text{Ga}]$ GaDFOSq-TIDE or  $[^{68}\text{Ga}]$ -GaDFOSq-TATE (2–3 MBq, 1  $\mu\text{g}$ , 0.5 nmol) and then euthanized at either 1 or 2 h after administration. The amount of injected activity per gram of tissue (%IA/g) in the tumor and major organs was quantified (Figure 4 and SI). At 1 h

post-injection, the tumor uptake of  $[^{68}\text{Ga}]$ GaDFOSq-TATE was  $9.80 \pm 2.33\% \text{IA/g}$  and administration of  $[^{68}\text{Ga}]$ -GaDFOSq-TIDE gave a tumor uptake of  $8.81 \pm 1.03\% \text{IA/g}$ . The initial tumor uptake of  $[^{68}\text{Ga}]$ GaDFOSq-TIDE reduced from  $8.81 \pm 1.03\% \text{IA/g}$  at 1 h post-injection to  $4.4 \pm 1.1\% \text{IA/g}$  at 2 h post-injection (Figure 4). In contrast, the tumor uptake of  $[^{68}\text{Ga}]$ GaDFOSq-TATE at 1 h post-injection ( $9.80 \pm 2.33\% \text{IA/g}$ ) is retained at 2 h post-injection ( $9.22 \pm 0.92\% \text{IA/g}$ ) consistent with the PET images (Figure 3).  $[^{68}\text{Ga}]$ -GaDFOSq-TIDE displays a higher degree of uptake in the kidneys (1 h,  $37.56 \pm 3.50\% \text{IA/g}$ ) than  $[^{68}\text{Ga}]$ GaDFOSq-TATE (1 h,  $15.98 \pm 3.27\% \text{IA/g}$ ).

$[^{89}\text{Zr}]$ ZrDFOSq-TATE and  $[^{89}\text{Zr}]$ ZrDFOSq-TIDE were evaluated in the same mouse model. The tracers (2–3 MBq, 6  $\mu\text{g}$ , 3.3 nmol) were administered via intravenous tail vein injection, and PET images were acquired at 1, 2, 4, and 18 h post-injection. Both tracers display rapid clearance from blood with low uptake in bone and muscle. At each time point, the tumor uptake of  $[^{89}\text{Zr}]$ ZrDFOSq-TATE (e.g., 1 h post-injection,  $\text{SUV}_{\text{max}} 3.1 \pm 0.24$ ) is higher than for  $[^{89}\text{Zr}]$ -ZrDFOSq-TIDE (e.g., 1 h post-injection  $\text{SUV}_{\text{max}} 1.1 \pm 0.07$ ). The coinjection of  $\sim 20$ -fold excess of the respective peptides (approximately 120  $\mu\text{g}$ , 66 nmol per mouse) results in a significant reduction in tumor uptake, suggesting the uptake of both tracers in the tumor is receptor mediated (Figure 5).

*Ex vivo* biodistribution studies (Figure 6) confirmed the observations made by inspection of the PET images. The tumor uptake of  $[^{89}\text{Zr}]$ ZrDFOSq-TATE (1 h,  $10.4 \pm 0.5\% \text{IA/g}$ ; 18 h  $4.9 \pm 0.8\% \text{IA/g}$ ) was higher than  $[^{89}\text{Zr}]$ ZrDFOSq-TIDE (1 h,  $3.4 \pm 0.4\% \text{IA/g}$ ; 18 h  $1.7 \pm 0.1\% \text{IA/g}$ ).  $[^{89}\text{Zr}]$ ZrDFOSq-TIDE has higher accumulation in the liver (1 h,  $10.8 \pm 0.4\% \text{IA/g}$ ) than  $[^{89}\text{Zr}]$ ZrDFOSq-TATE (1 h,  $4.3 \pm 0.4\% \text{IA/g}$ ). Both  $[^{89}\text{Zr}]$ ZrDFOSq-TATE (1 h,  $49.9 \pm 4.6\% \text{IA/g}$ ; and  $[^{89}\text{Zr}]$ ZrDFOSq-TIDE (1 h,  $39.79 \pm 1.8$ ) exhibit significant uptake in the kidneys.

## DISCUSSION

The iron(III) siderophore desferrioxamine B ( $\text{H}_3\text{DFO}$ ) forms stable complexes with both gallium(III),  $\log\beta_{\text{GaDFO}} 28.2$ ,<sup>36</sup> and zirconium(IV),  $\log\beta_{\text{ZrHDFO}} = 47.6$ .<sup>37</sup> Hexadentate DFO forms coordinatively saturated six-coordinate complexes with gallium(III), and both  $[^{68}\text{Ga}]$ GaDFOSq-TIDE and  $[^{68}\text{Ga}]$ -GaDFOSq-TATE are stable in the presence of human serum albumin. In contrast to the gallium(III) complex, the presence of a squaramide functional group in  $\text{H}_3\text{DFOSq}$ -conjugates may lead to either 7- or 8-coordinate to zirconium(IV) complexes where the dione backbone of the squaramide functional group also coordinates the metal ion. Analysis of a zirconium(IV) complex of a DFOSq-conjugate by  $^{13}\text{C}$  NMR spectroscopy suggested that the dione backbone does interact with the metal ion, whereas there are no such interactions in the analogous gallium(III) complex.<sup>27,34</sup> Predictive computational modeling of  $[\text{Zr}(\text{DFOSqOCH}_2\text{CH}_3)]^+$  with density functional theory suggested that one of the oxygen atoms of the dicarbonyl functional group bound to the zirconium(IV) ion.<sup>38</sup> Both  $[^{89}\text{Zr}]$ ZrDFOSq-TIDE and  $[^{89}\text{Zr}]$ ZrDFOSq-TATE are stable in the presence of human serum albumin.

A limitation of this study is that the relative binding affinities of each tracer to SSTR were not measured, but blocking studies in the mouse models demonstrated that it is highly likely that the tumor uptake is receptor-mediated. Furthermore, multiple studies have highlighted that the SSTR binding affinities of Tyr<sup>3</sup>-octreotide and Tyr<sup>3</sup>-octreotate are tolerant of

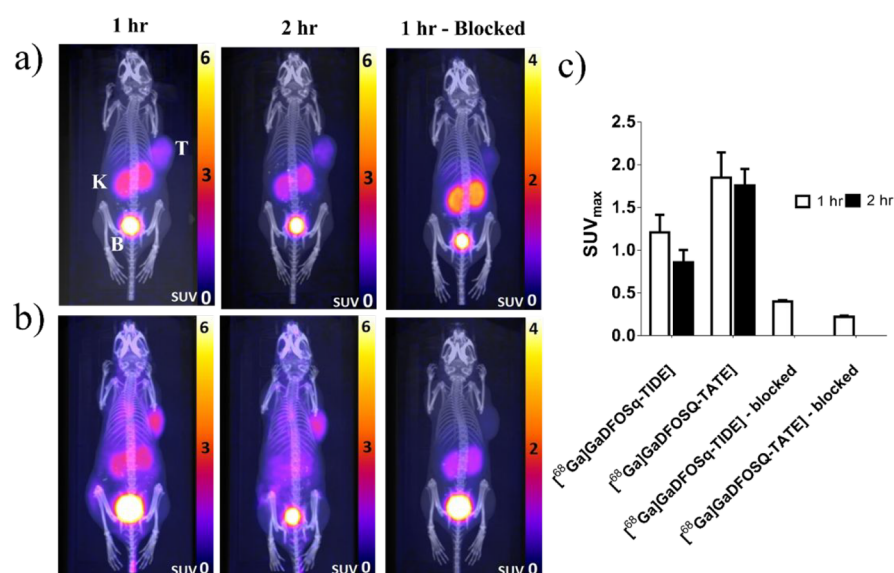


**Figure 3.** MicroPET maximum intensity projection (MIP) and CT images of mice bearing AR42J xenograft tumors injected with (a)  $[^{68}\text{Ga}]\text{GaDFOSq-TIDE}$  and (b)  $[^{68}\text{Ga}]\text{GaDFOSq-TATE}$  tracers at 1 and 2 h p.i.; (c) Tumor  $\text{SUV}_{\text{max}}$  analyzed from PET images and results are shown as mean  $\pm$  SEM,  $n = 3$ ; blocking was achieved by injecting excess amount of uncomplexed peptides. Organ labels: tumor (T), kidney (K), bladder (B).

modification at the *N*-terminus of the peptide with hydrophilic functional groups and metal complexes, although it was acknowledged that different metal complexes can lead to small changes to relative binding affinities for SSTR.<sup>1,3,16</sup> It is also significant that the higher measured affinity of  $[^{68}\text{Ga}]\text{GaDOTATATE}$  for SSTR2 ( $0.2 \pm 0.04$  nM) when compared to  $[^{68}\text{Ga}]\text{GaDOTATOC}$  ( $2.5 \pm 0.5$  nM)<sup>1</sup> did not prove to be clinically relevant in a comparative study in human subjects.<sup>39,40</sup> The Tyr<sup>3</sup>-octreotide and Tyr<sup>3</sup>-octreotate peptides were synthesized with the Lys<sup>5</sup> residue protected with a *t*-Boc group using standard solid-phase peptide synthesis methodologies. The peptides were attached to the chelator by reaction of  $\text{H}_3\text{DFOSqOEt}$  with peptide in solution at room temperature. Deprotection of the *t*-Boc protecting from the Lys<sup>5</sup> residue allowed isolation of  $\text{H}_3\text{DFOSq-TATE/TIDE}$  in  $\sim 25\text{--}28\%$  yield.

The new DFOSq conjugates could be radiolabeled with gallium-68 in  $\geq 98\%$  radiochemical yield at room temperature in 10 min using relatively low amounts of peptide ( $\sim 150$  ng/MBq, 0.08 nmol/MBq of  $[^{68}\text{Ga}]\text{Ga}^{\text{III}}$ ). It was also possible to radiolabel  $\text{H}_3\text{DFOSq-TATE/TIDE}$  with zirconium-89 at room temperature with radiochemical yields of  $>95\%$  with 2  $\mu\text{g}$  of ligand/MBq (1.1 nmol/MBq). Purification with a C18 cartridge allowed isolation of  $[^{89}\text{Zr}]\text{ZrDFOSq-TIDE}$  and  $[^{89}\text{Zr}]\text{ZrDFOSq-TATE}$  in  $>98\%$  radiochemical purity. The radiochemical procedures reported here are similar to our previous work on  $\text{H}_3\text{DFOSq-glutamate-ureido-lysine}$  derivatives.<sup>27</sup> The initial radiolabeling with both gallium-68 and zirconium-89 was conducted at ambient temperature, but it is likely that heating the reaction mixtures to  $\sim 75$   $^\circ\text{C}$  would further decrease the amount of peptide required to obtain high radiochemical yields leading to higher specific activities, and this will be investigated in further work. All four complexes have similar lipophilicities, as estimated by their distribution coefficients ( $\text{Log } D_{7.4}$ ), which range from  $-0.88 \pm 0.06$  for  $[^{89}\text{Zr}]\text{ZrDFOSq-TATE}$  to  $-1.38 \pm 0.07$  for  $[^{68}\text{Ga}]\text{GaDFOSq-TATE}$  (Table 1).

All four tracers were evaluated in a murine xenograft model using a neuroendocrine tumor cell line with endogenous expression of SSTR2 (AR42J). The PET images acquired following injection of either  $[^{68}\text{Ga}]\text{GaDFOSq-TIDE}$  or  $[^{68}\text{Ga}]\text{GaDFOSq-TATE}$  (Figure 3) show that the tumor uptake of the latter is marginally higher than the former, but both tracers produce images with high tumor uptake. As expected, both tracers have significant uptake in the kidneys and bladder, consistent with the renal excretion expected for peptides. The PET images following administration of  $[^{68}\text{Ga}]\text{GaDFOSq-TATE}$  display evidence of some activity remaining in the blood resulting in a blood pool background signal from the left ventricle of the heart (Figure 3). The higher activity in blood following administration of  $[^{68}\text{Ga}]\text{GaDFOSq-TATE}$  when compared to  $[^{68}\text{Ga}]\text{GaDFOSq-TIDE}$  was confirmed by the *ex vivo* biodistribution study, but the reason for this difference is known (Figure 4). The specificity of the receptor-mediated uptake in the tumor was supported by a blocking study where addition of an excess of the respective nonradioactive peptide-DFOSq conjugates leads to a significant reduction in tumor uptake (Figure 3a). The higher tumor uptake of  $[^{68}\text{Ga}]\text{GaDFOSq-TATE}$  at 1 h post-injection ( $9.80 \pm 2.33\%$ IA/g) is retained at 2 h post-injection ( $9.22 \pm 0.92\%$ IA/g). In contrast, the tumor uptake of  $[^{68}\text{Ga}]\text{GaDFOSq-TIDE}$  reduced from  $8.81 \pm 1.03\%$ IA/g at 1 h post-injection to  $4.4 \pm 1.1\%$ IA/g at 2 h post-injection (Figure 4). In an early demonstration of the potential of DFO to act as a ligand for gallium-67 and gallium-68, the ligand was coupled to octreotide through a succinyl linker. The gallium-67/68 complexes were stable *in vivo* and displayed rapid tumor uptake in Islet Cell tumor-bearing rats with  $0.56\%$ IA/g accumulating in the tumor at 1 h post-injection.<sup>29</sup>

Direct comparisons with the tumor uptake of  $[^{68}\text{Ga}]\text{GaDFOSq-TATE}$  with that of  $[^{68}\text{Ga}]\text{GaDOTATATE}$  in AR42J tumor xenograft models need to be approached with caution, because reported values vary widely, presumably because the size of the respective tumors, the amount of peptide injected, and the mouse strain used can affect the

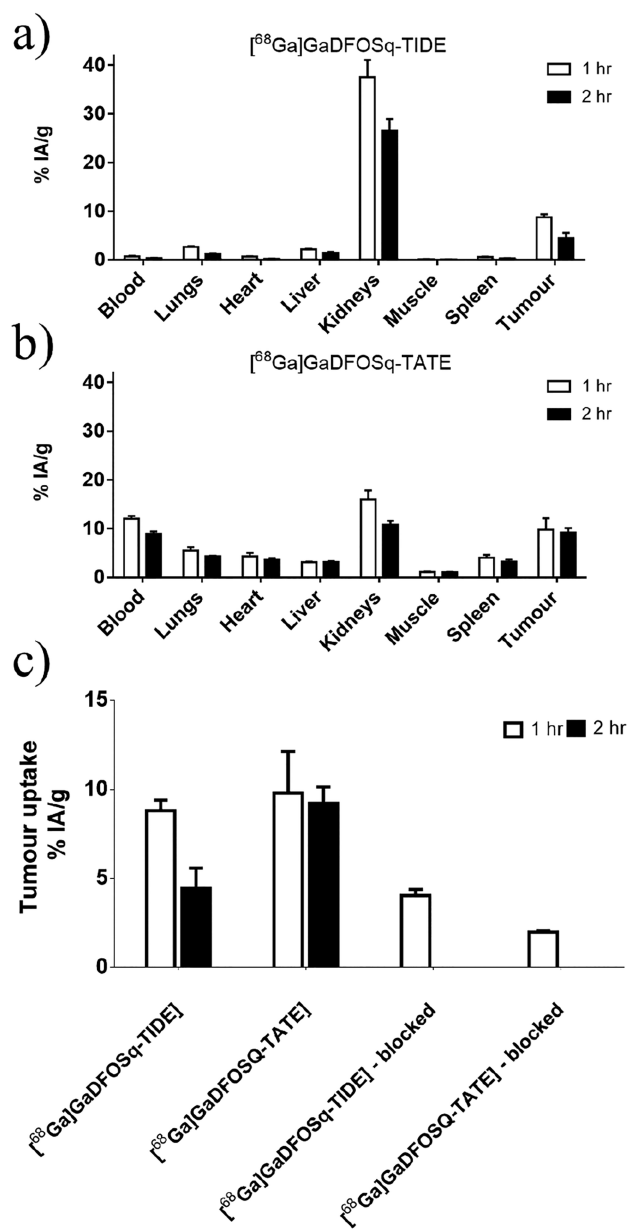


**Figure 4.** *Ex vivo* biodistribution analysis, mice were euthanized at either 1 or 2 h after injection of either  $[^{68}\text{Ga}]\text{GaDFOSq-TIDE}$  (a) or  $[^{68}\text{Ga}]\text{GaDFOSq-TATE}$  (b). Tumor uptake of  $[^{68}\text{Ga}]\text{GaDFOSq-TIDE}$  and  $[^{68}\text{Ga}]\text{GaDFOSq-TATE}$  and reduction in tumor uptake following “blocking” by injecting excess peptide conjugate (c). Tracer uptake is expressed as percent injected activity/gram of tumor, data represents mean  $\pm$  SEM of  $n = 3$  mice/group.

degree of uptake. In previous work, in the same AR42J tumor xenograft model from our laboratory the tumor uptake of  $[^{68}\text{Ga}]\text{GaDOTATATE}$  was  $14.4 \pm 0.8\% \text{IA/g}$ .<sup>41</sup> In another example, the tumor uptake of  $[^{68}\text{Ga}]\text{GaDOTATATE}$  in AR42J tumor xenograft models was  $3.14 \pm 2.07\% \text{IA/g}$  at 1 h post-injection,<sup>42</sup> but higher tumor uptakes of  $24.1 \pm 4.9$  and  $21.6 \pm 4\% \text{IA/g}$  have also been reported.<sup>43,44</sup>

The PET images in the AR42J xenograft model following injection of both  $[^{89}\text{Zr}]\text{ZrDFOSq-TIDE}$  and  $[^{89}\text{Zr}]\text{ZrDFOSq-TATE}$  show that both tracers provide images with high uptake in tumor and very low background. The tumor uptake of  $[^{89}\text{Zr}]\text{ZrDFOSq-TATE}$  is higher than for  $[^{89}\text{Zr}]\text{ZrDFOSq-TIDE}$ , and there is a larger difference between the different

peptides than for the gallium-68 analogues. This difference in tumor uptake is confirmed by the *ex vivo* biodistribution studies. Two other positron-emitting radionuclides with radioactive half-lives that are compatible with centralized manufacture are copper-64 ( $t_{1/2} \sim 12.7$  h) and fluorine-18 ( $t_{1/2} \sim 109$  min). Direct comparisons of tumor uptake from independent studies have to be approached with caution due to likely differences in tumor size, the amount of agent used, and the different time points used. The tumor uptake of  $[^{89}\text{Zr}]\text{ZrDFOSq-TATE}$  ( $10.4 \pm 0.5\% \text{IA/g}$  at 1 h post-injection) is less than that of a fluorine agent,  $\text{Al-}[^{18}\text{F}]\text{F-NOTA-octreotide}$  (NOTA = 1,4,7-triazacyclononane-1,4,7-triacetic acid) in the same AR42J tumor model ( $28.3 \pm 5.7\% \text{ID/g}$  at 2 h after injection)<sup>15</sup> and  $[^{64}\text{Cu}]\text{CuSarTATE}$ , a copper complex conjugated to octreotate, which has a tumor uptake of  $61.8 \pm 2.4\% \text{IA/g}$  4 h after injection in AR42J tumors.<sup>20</sup>

The images show that administration of  $[^{89}\text{Zr}]\text{ZrDFOSq-TIDE}$  leads to higher liver uptake when compared to administration of  $[^{89}\text{Zr}]\text{ZrDFOSq-TATE}$ , suggesting more hepatobiliary clearance for the former. The images acquired following administration of  $[^{89}\text{Zr}]\text{ZrDFOSq-TATE}$  do show uptake in the gallbladder (particularly at 2 h post-injection), and some activity in liver and bowel (with likely radioactive faeces at the 4 h time point) indicative of some hepatobiliary excretion. There is little evidence of radioactivity in bone in the PET images, and this is confirmed in the *ex vivo* biodistribution suggesting the zirconium-89 complexes are stable *in vivo*. The differing biodistribution and clearance mechanisms of the gallium-68 and zirconium-89 labeled versions of each tracer and especially the higher kidney uptake of the zirconium complexes can at least partially be attributed to the different ionic charges of the metal ion ( $\text{Ga}^{\text{III}}$  versus  $\text{Zr}^{\text{IV}}$ ).

## CONCLUSIONS

The peptides Tyr<sup>3</sup>-octreotide and Tyr<sup>3</sup>-octreotate that bind to SSTR were conjugated to DFOSq. The new ligands can be radiolabeled with either gallium-68 or zirconium-89 at room temperature to give the radioactive complexes in high radiochemical yield. All four agents displayed good tumor uptake and produced good quality PET images in an AR42J xenograft model that has endogenous expression of SSTR2. For both radionuclides, the complexes formed with DFOSq-TATE performed better, with higher tumor uptake and retention, than the complexes formed with DFOSq-TIDE. The quality of the PET images acquired following administration of  $[^{89}\text{Zr}]\text{ZrDFOSq-TATE}$  suggests further studies on the potential of this agent are warranted. These studies should include prospective dosimetry to assess the potential radiation dose to nontarget organs such as the kidneys as well as more thorough investigations of the stability of the complexes when prepared with high levels of radioactivity. The versatile ligands presented here can be radiolabeled with either gallium-68 or zirconium-89 at room temperature, and in principle, this chemistry could be readily translated to kit-based formulations. The long radioactive half-life of zirconium-89 makes distribution of presynthesized tracers to sites that lack the capability for on-site production of gallium-68 tracers feasible.

## MATERIAL AND METHODS

**General Experimental and Materials.** Reagents were purchased from commercial sources.  $\text{H}_3\text{DFOSq}$  was synthesized by a reported procedure.<sup>34</sup> Gallium-68 was eluted with

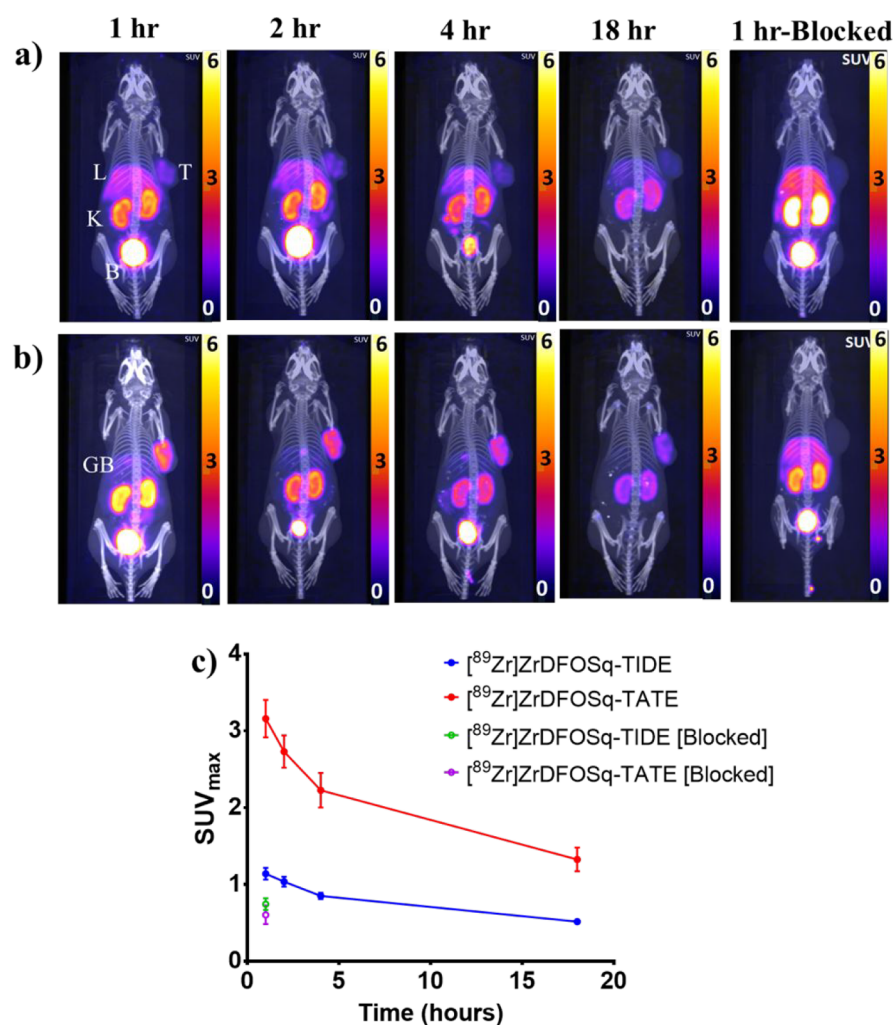


**Figure 5.** MicroPET (MIP) and CT images of mice bearing AR42J xenograft tumors after 1, 2, 4, and 18 h post-injection of (a)  $[^{89}\text{Zr}]ZrDFOSq-TIDE$  and (b)  $[^{89}\text{Zr}]ZrDFOSq-TATE$  tracers; (c) Time activity curves for tumor  $SUV_{max}$  analyzed from PET images, and results are shown as mean  $\pm$  SEM,  $n = 3$  ( $n = 4$  for blocking experiment; blocking was achieved by injecting an  $\sim 20$ -fold excess of either  $H_3DFOSq-TIDE$  or  $H_3DFOSq-TATE$ ). Organ labels: tumor (T), liver (L), kidneys (K), bladder (B), and gallbladder (GB).

hydrochloric acid (0.05 M, 4 mL) from a 1850 MBq Ge-68/Ga-68 Generator from ITG Isotope Technologies Garching GmbH. Zirconium-89 was obtained from either PerkinElmer Inc. (part #NEZ308000MC) or the Department of Molecular Imaging and Therapy, Austin Health). ESI-MS spectra were recorded on Thermo Fisher OrbiTRAP infusion mass spectrometer. For details of HPLC conditions, see [Supporting Information](#).

**Synthesis of Lysine Side Chain Protected Tyr<sup>3</sup>-Octreotide/Octreotate Peptides.** Tyr<sup>3</sup>-octreotide or Tyr<sup>3</sup>-octreotate linear peptide with sequence [DPhe-Cys(Acm)-Tyr(*t*Bu)-D(Trp)-Lys(Boc)-Thr(*t*Bu)-Cys(Acm)-Thr(*t*Bu)-OL or OH] were prepared using a CEM Liberty Blue automated microwave peptide synthesizer. For the octreotate peptide, Fmoc-Thr(*t*Bu)-OH preloaded on Wang resin was used, while for octreotide, preloaded Fmoc-Threninol(*t*Bu) on 2-chlorotrityl resin was used. Each coupling cycle involved HATU (1 equiv) and DIPEA (5 equiv) followed by deprotection of Fmoc group using 20% piperidine in DMF, but no final deprotection of N-terminal Fmoc group was performed. The resin-bound linear peptides were cyclized using iodine (1 mg/mg of resin) in DMF (20 mL). The resin cleavage was performed using a solution of triisopropylsilane (2.5%),

distilled water (2.5%), 3,6-dioxa-1,8-octanedithiol (2.5%), and thioanisole (2.5%) in TFA (5 mL) with gentle shaking for 2 h at RT. The resin was filtered, and the filtrate was sparged with  $N_2$  to reduce the volume to 1 mL, and then diethyl ether (40 mL) was added to precipitate the peptide which was collected after centrifugation. The crude cyclic peptides Fmoc-TATE/TIDE were purified by HPLC (Phenomenex Luna 5  $\mu\text{m}$  C18(2) 100 Å, LC column 250  $\times$  21 mm using 0.1% TFA in Milli-Q water and acetonitrile), and the identity of the peptides were confirmed by ESI-MS. The purified cyclic peptides Fmoc-TATE/TIDE were dissolved in DMF (1 mL) and treated with di-*tert*-butyldicarbonate (5 equiv) in the presence of DIPEA (1 equiv) for 4 h at RT, and then cold diethyl ether was added to the reaction mixture to precipitate the product which was collected by centrifugation. The residue was treated with 20% piperidine in DMF (1 mL) for 30 min at RT and then precipitated again with cold diethyl ether, and the residue was collected by centrifugation and purified by HPLC (Column C, SI) to provide the peptides Lys(*t*-Boc)-TATE/TIDE. Analytical HPLC was performed (Column B, SI) and HPLC purity found to be >95% for both peptides. ESI-MS: Lys(*t*-Boc)-TIDE (+ve ion)  $[M + H^+]$   $m/z = 1135.4952$  (experimental), calculated for

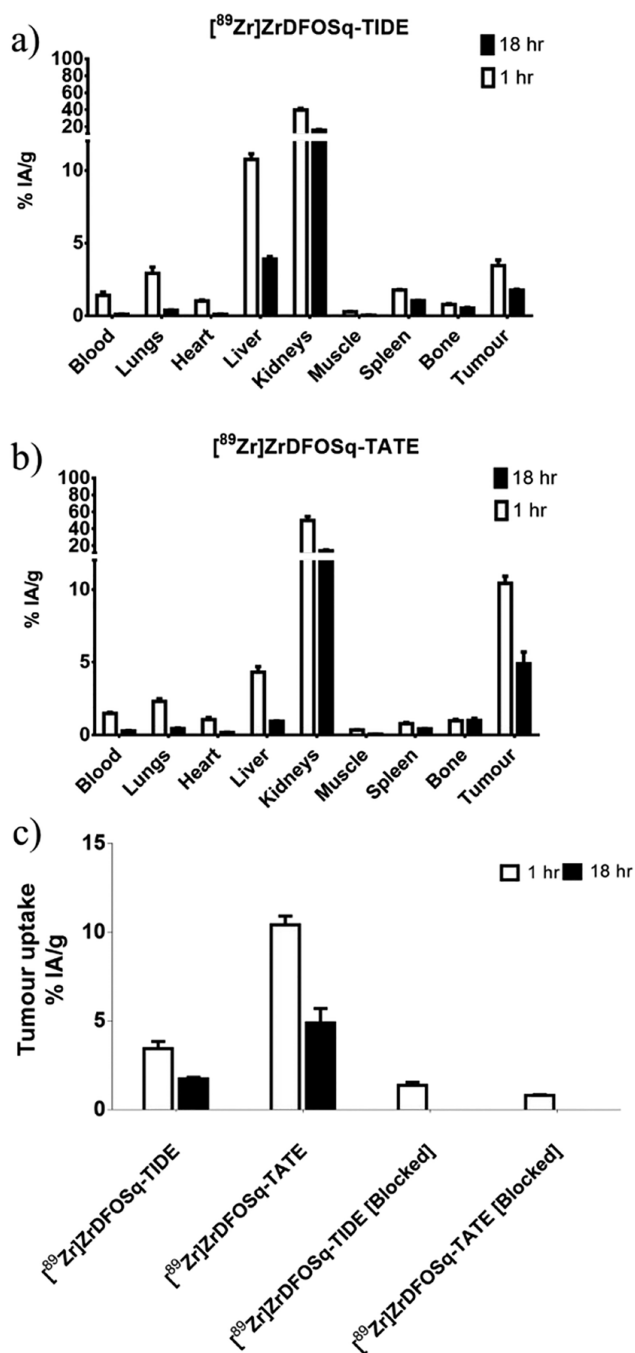


**Figure 6.** *Ex vivo* biodistribution analysis at 1 and 18 h after injection with either [<sup>89</sup>Zr]ZrDFOSq-TIDE (a) or [<sup>89</sup>Zr]ZrDFOSq-TATE (b). Tracer uptake is expressed as percent injected activity/gram tissue. Data represents mean ± SEM of *n* = 3 mice/group. (c) Tumor uptake following injection of either [<sup>89</sup>Zr]ZrDFOSq-TIDE or [<sup>89</sup>Zr]-ZrDFOSq-TATE and “blocking” experiment, with ~20-fold excess of respective peptide conjugate, data represents mean ± SEM of *n* = 4 mice/group.

[C<sub>54</sub>H<sub>75</sub>N<sub>10</sub>O<sub>13</sub>S<sub>2</sub>]<sup>+</sup>: *m/z* = 1135.4956; Lys(*t*-Boc)TATE (+ve ion) [M + H<sup>+</sup>] *m/z* = 1149.4739 (experimental), calculated for [C<sub>54</sub>H<sub>73</sub>N<sub>10</sub>O<sub>14</sub>S<sub>2</sub>]<sup>+</sup>: *m/z* = 1149.4749.

**Synthesis of H<sub>3</sub>DFOSq-TATE/TIDE.** Lys(*t*-Boc)-TATE/TIDE (1 equiv) and DFOSq (5 equiv) were dissolved in DMSO (100 μL), and then borate buffer (0.1 M, pH 9.0, 900 μL) was added. The solution was slowly agitated at room

**Table 1.** Log *D*<sub>7.4</sub> for [<sup>89</sup>Zr]ZrDFOSq-TATE/TIDE and [<sup>68</sup>Ga]GaDFOSq-TATE/TIDE

Complex	Log <i>D</i> <sub>7.4</sub>
[ <sup>89</sup> Zr]ZrDFOSq-TIDE	-1.03 ± 0.13
[ <sup>89</sup> Zr]ZrDFOSq-TATE	-0.88 ± 0.06
[ <sup>68</sup> Ga]GaDFOSq-TIDE	-0.98 ± 0.07
[ <sup>68</sup> Ga]GaDFOSq-TATE	-1.38 ± 0.07

temperature for 7 days, and then neutralized with 10% TFA and purified by HPLC (Column C, SI) and the identity of peptides were confirmed by ESI-MS. The purified fractions were treated with 20% TFA in DCM for 30 min at RT, and then TFA was removed under N<sub>2</sub> flow followed by HPLC purification again. Analytical HPLC was performed (Columns A and B, SI) and HPLC purity found to be >95% for both peptides. ESI-MS: H<sub>3</sub>DFOSq-TIDE (+ve ion) [M + H<sup>+</sup>] *m/z* = 1673.7716 (experimental), calculated for [C<sub>78</sub>H<sub>113</sub>N<sub>16</sub>O<sub>21</sub>S<sub>2</sub>]<sup>+</sup>: *m/z* = 1673.7708; H<sub>3</sub>DFOSq-TATE (+ve ion) [M + H<sup>+</sup>] *m/z* = 1687.7500 (experimental), calculated for [C<sub>78</sub>H<sub>111</sub>N<sub>16</sub>O<sub>22</sub>S<sub>2</sub>]<sup>+</sup>: *m/z* = 1687.7500.

**Synthesis of [<sup>68</sup>Ga]GaDFOSq-TIDE.** <sup>68</sup>Ga<sup>III</sup> in HCl (630 μL, 44 MBq) was buffered with sodium acetate (1 M, 70 μL, pH 4.5), then H<sub>3</sub>DFOSq-TIDE (6 μg in 6 μL DMSO, 3.3 nmol), and the reaction mixture was left to stand at room temperature for 15 min; then, an aliquot was analyzed by radio-HPLC (Column B, SI). The traces showed >98% radiochemical yield with a radiochemical purity of >98%. The reaction mixture was diluted with Milli-Q water (470 μL) and then buffered with 10 × PBS buffer (130 μL, pH 7.4) to a final volume of 1.3 mL. Six syringes (BD Ultra-Fine, 0.3 mL) containing approximately 3.5 MBq in 200 μL (approximately peptide mass 1 μg, 0.5 nmol) were prepared. An excess of H<sub>3</sub>DFOSq-TIDE (~20 equiv, approximately 20 μg, 11 nmol per mouse) was added to each injection for the “blocking” experiment.

**Synthesis of [<sup>68</sup>Ga]GaDFOSq-TATE.** <sup>68</sup>Ga<sup>III</sup> in HCl (900 μL, 40 MBq) was buffered with sodium acetate (1 M, 100 μL, pH 4.5), then H<sub>3</sub>DFOSq-TATE (6 μg in 6 μL DMSO, 3.3 nmol), and the reaction mixture was left to stand at room temperature for 15 min; then, an aliquot was analyzed by radio-HPLC (Column B, SI). The traces showed >95% radiochemical yield with a radiochemical purity of >95%. The reaction mixture was diluted with Milli-Q water (100 μL) and then buffered with 10 × PBS buffer (110 μL, pH 7.4) to a final volume of 1.2 mL. Six syringes (BD Ultra-Fine, 0.3 mL) containing approximately 2.3 MBq in 200 μL (approximately peptide mass 1.0 μg, 0.5 nmol) were prepared. An excess of H<sub>3</sub>DFOSq-TATE (~20 equiv, approximately 20 μg, 11.1 nmol per mouse) was added to each injection for the “blocking” experiment.

**Synthesis of [<sup>89</sup>Zr]ZrDFOSq-TIDE.** <sup>89</sup>Zr<sup>IV</sup> in 1 M oxalic acid (60 μL, 60 MBq) was diluted with Milli-Q water (60 μL) and then was neutralized (pH 6–7) with a series of small volume additions of aqueous Na<sub>2</sub>CO<sub>3</sub> (1 M, 4 × 10 μL). HEPES buffer (54 μL, 1 M, pH 7.0) was then added and the solution allowed to stand for 5 min before pH was tested again. After confirming the mixture had a pH 6–7, a solution of H<sub>3</sub>DFOSq-TIDE (120 μg in 60 μL of 0.25 M HEPES buffer, 10% DMSO, 1.18 nmol/MBq) was added, and the reaction mixture was left to stand at room temperature for 30 min; then, an aliquot was analyzed by radio-HPLC (Column B, SI). The crude tracer was purified by Phenomenex StrataX

cartridges (C18, 60 mg) using ethanol as eluent, and fractions containing most labeled product (30 MBq) were combined and diluted to 8% ethanol in PBS to final volume of 1.0 mL. The purified tracer was analyzed by radio-HPLC (Column B, SI) and radiochemical purity of the tracer found to be >95%. Six syringes (BD Ultra-Fine, 0.3 mL) containing approximately 2–3 MBq (approximately peptide mass 6  $\mu\text{g}$ , 3.3 nmol) in 165  $\mu\text{L}$  were prepared. An excess of H<sub>3</sub>DFOSq-TIDE (~20 equiv, approximately 120  $\mu\text{g}$ , 66 nmol per mouse) was added to each injection for the “blocking” experiment.

**Synthesis of [<sup>89</sup>Zr]ZrDFOSq-TATE.** <sup>89</sup>Zr<sup>IV</sup> in 1 M oxalic acid (70  $\mu\text{L}$ , 56 MBq) was diluted with Milli-Q water (70  $\mu\text{L}$ ) and then was neutralized (pH 6–7) with a series of small volume additions of aqueous Na<sub>2</sub>CO<sub>3</sub> (1 M, 4  $\times$  10  $\mu\text{L}$ ). HEPES buffer (62  $\mu\text{L}$ , 1 M, pH 7.0) was then added and the solution allowed to stand for 5 min before pH was tested again. After confirming the mixture had a pH 6–7, a solution of H<sub>3</sub>DFOSq-TATE (112  $\mu\text{g}$  in 56  $\mu\text{L}$  of 0.25 M HEPES buffer, 10% DMSO, 1.19 nmol/MBq) was added into the <sup>89</sup>Zr<sup>IV</sup> solution, and the reaction mixture was left to stand at room temperature for 30 min; then, an aliquot was analyzed by radio-HPLC (Column B, SI). The crude tracer was purified by Phenomenex StrataX cartridges (C18, 60 mg) using ethanol as eluent, and fractions containing most labeled product (28.8 MBq) were combined and diluted to 8% ethanol in PBS to final volume of 1.0 mL. The purified tracer was analyzed by radio-HPLC, and radiochemical purity of the tracer was found to be >95%. Six syringes (BD Ultra-Fine, 0.3 mL) containing approximately 2–3 MBq (approximately peptide mass 6  $\mu\text{g}$ , 3.3 nmol) in 150  $\mu\text{L}$  were prepared. An excess of H<sub>3</sub>DFOSq-TATE (~20 equiv, approximately 120  $\mu\text{g}$ , 66 nmol per mouse) was added to each injection for the “blocking” experiment.

**Synthesis of [<sup>nat</sup>Ga]GaDFOSq-TATE.** A solution of H<sub>3</sub>DFOSq-TATE (1 mg, 0.592  $\mu\text{mol}$ ) and Ga(NO<sub>2</sub>)<sub>3</sub>·H<sub>2</sub>O (0.2 mg, 0.9  $\mu\text{mol}$ ) in acetonitrile:water (1:1, 500  $\mu\text{L}$ ) was stirred for 2 h at room temperature and then purified by HPLC. The purified fractions were analyzed by analytical HPLC and HRMS. ESI-MS: [<sup>nat</sup>Ga]GaDFOSq-TATE (+ve ion) [M + 2H<sup>+</sup>]  $m/z$  = 878.3280 (experimental), calculated for [C<sub>78</sub>H<sub>109</sub>Ga<sub>1</sub>N<sub>16</sub>O<sub>22</sub>S<sub>2</sub>]<sup>2+</sup>:  $m/z$  = 878.3300.

**Synthesis of [<sup>nat</sup>Ga]GaDFOSq-TIDE.** A solution of H<sub>3</sub>DFOSq-TIDE (1 mg, 0.597  $\mu\text{mol}$ ) and Ga(NO<sub>2</sub>)<sub>3</sub>·H<sub>2</sub>O (0.2 mg, 0.9  $\mu\text{mol}$ ) in acetonitrile:water (1:1, 500  $\mu\text{L}$ ) was stirred for 2 h at room temperature and then purified by HPLC. The purified fractions were analyzed by analytical HPLC and HRMS. ESI-MS: [<sup>nat</sup>Ga]GaDFOSq-TIDE (+ve ion) [M + 2H<sup>+</sup>]  $m/z$  = 871.3393 (experimental), calculated for [C<sub>78</sub>H<sub>111</sub>Ga<sub>1</sub>N<sub>16</sub>O<sub>21</sub>S<sub>2</sub>]<sup>2+</sup>:  $m/z$  = 871.3331.

**Synthesis of [<sup>nat</sup>Zr]ZrDFOSq-TATE.** A solution of H<sub>3</sub>DFOSq-TATE (1 mg, 0.592  $\mu\text{mol}$ ) and ZrCl<sub>4</sub>·2THF (0.8 mg, 2.3  $\mu\text{mol}$ ) in acetonitrile:water (1:1, 500  $\mu\text{L}$ ) was stirred for 2 h at room temperature and then purified by HPLC. The purified fractions were analyzed by analytical HPLC and HRMS. ESI-MS: [<sup>nat</sup>Zr]ZrDFOSq-TATE (+ve ion) [M + 2H<sup>+</sup>]  $m/z$  = 887.8199 (experimental), calculated for [C<sub>78</sub>H<sub>109</sub>N<sub>16</sub>O<sub>22</sub>S<sub>2</sub>Zr]<sup>2+</sup>:  $m/z$  = 887.8190.

**Synthesis of [<sup>nat</sup>Zr]ZrDFOSq-TIDE.** A solution of H<sub>3</sub>DFOSq-TIDE (1 mg, 0.597  $\mu\text{mol}$ ) and ZrCl<sub>4</sub>·2THF (0.9 mg, 2.3  $\mu\text{mol}$ ) in acetonitrile:water (1:1, 500  $\mu\text{L}$ ) was stirred for 2 h at room temperature and then purified by HPLC. The purified fractions were analyzed by analytical HPLC and HRMS. ESI-MS: [<sup>nat</sup>Zr]ZrDFOSq-TATE (+ve ion) [M +

2H<sup>+</sup>]  $m/z$  = 880.8249 (experimental), calculated for [C<sub>78</sub>H<sub>111</sub>N<sub>16</sub>O<sub>21</sub>S<sub>2</sub>Zr]<sup>2+</sup>:  $m/z$  = 880.8293.

**Measurement of Log(D<sub>7,4</sub>).** Radioactive reaction mixture (10  $\mu\text{L}$  aliquot) was added to 1-octanol (500  $\mu\text{L}$ , saturated with PBS) and PBS (490  $\mu\text{L}$ , saturated with 1-octanol). The mixture was mixed and then allowed to separate (30 min). A portion (400  $\mu\text{L}$ ) from 1-octanol layer was repartitioned against PBS (400  $\mu\text{L}$ ). A portion (2  $\mu\text{L}$ ) of each layer was collected, and the radioactivity in each layer was quantified. Log D<sub>7,4</sub> = log<sub>10</sub> of the ratio of the counts between the 1-octanol layer and the PBS layer (each partition was repeated in three times (mean  $\pm$  SEM)).

**Stability of Radiolabeled Peptides in PBS and in the Presence of Human Serum Albumin.** The radiolabeled peptides were incubated at room temperature in phosphate buffered saline for 96 h for <sup>89</sup>Zr labeled peptides (2.5 MBq in 220  $\mu\text{L}$ ) and for 4 h for <sup>68</sup>Ga labeled peptides (18 MBq in 100  $\mu\text{L}$ ) and analyzed by radio-HPLC. To assess the stability of the [<sup>68</sup>Ga]GaDFOSq-TIDE/TATE and [<sup>89</sup>Zr]ZrDFOSq-TIDE/TATE in human serum albumin the complexes (10 MBq in ~50  $\mu\text{L}$ ) were incubated in 2% human serum in PBS for 3 h at 37 °C, and then an equal volume of acetonitrile was added to precipitate proteins. The precipitated proteins were separated by centrifugation and the supernatant was analyzed by radio-HPLC. The chromatograms (Figures S11–12, SI) reveal <5% decomposition to more hydrophilic uncharacterized compounds with shorter retention times, presumably due to radiolysis.

**Stability of [<sup>89</sup>Zr]ZrDFOSq-TATE with Respect to Radiolysis at Higher Activities (100 MBq).** <sup>89</sup>Zr<sup>IV</sup> (162  $\mu\text{L}$ , 100 MBq, in 0.05 M oxalic acid, produced by Department of Molecular Imaging and Therapy, Austin Health) was neutralized to pH 4.5 with sodium acetate (1 M, 187  $\mu\text{L}$ ), and then H<sub>3</sub>DFOSq-TATE (2.5  $\mu\text{g}$ , 1.5 nmol, in 1:1 Milli-Q:ethanol (25  $\mu\text{L}$ )) was added and the reaction mixture was agitated at 75 °C for 15 min. The reaction mixture was analyzed by radio-HPLC (Column B, SI). The traces showed >98% radiochemical yield with a radiochemical purity of >98%. Ethanol (48  $\mu\text{L}$ ), sodium gentisate (60  $\mu\text{L}$ , 5%), PBS (60  $\mu\text{L}$ ), and Milli-Q water (58  $\mu\text{L}$ ) were added to give a final volume of ~600  $\mu\text{L}$  (25 ng/MBq, 0.015 nmol/MBq in PBS with 10% ethanol and 0.5% Na-Gentisate). The stability of [<sup>89</sup>Zr]-ZrDFOSq-TATE was monitored by radio-HPLC showing that after 5 days >75% [<sup>89</sup>Zr]ZrDFOSq-TATE remained with evidence of one major unidentified decomposition product with a shorter retention time presumably due to a more hydrophilic species (Figure S13, SI).

**PET-CT Imaging and Biodistribution.** These tests were performed as reported previously<sup>27</sup> and are also included in the Supporting Information.

## ■ ASSOCIATED CONTENT

### SI Supporting Information

The Supporting Information is available free of charge at <https://pubs.acs.org/doi/10.1021/acs.bioconjchem.1c00109>.

HPLC information, information on animal experiments, additional figures for MS spectra; selected HPLC traces and microPET images for *in vivo* experiments (PDF)

## AUTHOR INFORMATION

### Corresponding Author

Paul S. Donnelly – School of Chemistry, University of Melbourne, Parkville, Victoria 3010, Australia; [orcid.org/0000-0001-5373-0080](https://orcid.org/0000-0001-5373-0080); Email: [pauld@unimelb.edu.au](mailto:pauld@unimelb.edu.au)

### Authors

Asif Noor – School of Chemistry, University of Melbourne, Parkville, Victoria 3010, Australia

Jessica K. Van Zuylenkom – Research Division, Peter MacCallum Cancer Centre, Melbourne, Victoria 3000, Australia

Stacey E. Rudd – School of Chemistry, University of Melbourne, Parkville, Victoria 3010, Australia

Peter D. Roselt – Centre for Cancer Imaging, Peter MacCallum Cancer Centre, Melbourne, Victoria 3000, Australia

Mohammad B. Haskali – Centre for Cancer Imaging, Peter MacCallum Cancer Centre, Melbourne, Victoria 3000, Australia; [orcid.org/0000-0003-3084-2084](https://orcid.org/0000-0003-3084-2084)

Eddie Yan – Telix Pharmaceuticals Limited, North Melbourne, Victoria 3051, Australia

Michael Wheatcroft – Telix Pharmaceuticals Limited, North Melbourne, Victoria 3051, Australia

Rodney J. Hicks – Research Division, Peter MacCallum Cancer Centre, Melbourne, Victoria 3000, Australia; Sir Peter MacCallum Department of Oncology, University of Melbourne, Parkville, Victoria 3010, Australia

Carleen Cullinane – Research Division, Peter MacCallum Cancer Centre, Melbourne, Victoria 3000, Australia; Sir Peter MacCallum Department of Oncology, University of Melbourne, Parkville, Victoria 3010, Australia

Complete contact information is available at:

<https://pubs.acs.org/10.1021/acs.bioconjchem.1c00109>

### Author Contributions

The manuscript was written through contributions of all authors. All authors have given approval to the final version of the manuscript.

### Notes

The authors declare the following competing financial interest(s): Asif Noor, Stacey E. Rudd and Paul S. Donnelly are listed as inventors on intellectual property relating to this research that has been licensed from the University of Melbourne to Telix Pharmaceuticals. Rodney Hicks has shares in Telix Radiopharmaceuticals that are held on behalf of the Peter MacCallum Cancer Centre. Michael Wheatcroft and Eddie Yan are employed by Telix Pharmaceuticals, the licensee of the intellectual property related to this research.

## ACKNOWLEDGMENTS

Telix Pharmaceuticals and the National Health and Medical Research Council, Australia (funding to Paul S. Donnelly, Carleen Cullinane, and Peter D. Roselt) for financial support. Australian Cancer Research Foundation supported the purchase of the PET/CT scanner used in this work. Susan Jackson (Peter MacCallum Cancer Centre) for expert technical assistance and Dr. Benjamin Blyth (Peter MacCallum Cancer Centre) for assistance with the blocking study experiments. Mass Spectrometry and Proteomics Facility (MSPF) (Bio21 Institute, University of Melbourne).

## ABBREVIATIONS USED

PET, positron emission tomography; SPECT, single photon emission computed tomographic; SSTR, somatostatin receptor; PRRT, peptide receptor radionuclide therapy; %IA/g, % injected activity per gram of tissue; %AR/g, % added activity per gram of tissue; H<sub>3</sub>DFO, desferrioxamine B; DOTA, 1,4,7,10-tetraazacyclododecane-1,4,7,10-tetraacetic acid; keV, kilo electronvolt; HATU, 1-[bis(dimethylamino)methylene]-1H-1,2,3-triazolo[4,5-b]pyridinium 3-oxide hexafluorophosphate; DIPEA, diisopropylamine; TFA, trifluoroacetic acid; MBq, mega becquerel; MIP, maximum intensity projection; SEM, standard error of the mean; SUV<sub>max</sub>, standardized uptake value; Log D<sub>7.4</sub>, distribution coefficient at pH 7.4

## REFERENCES

- (1) Reubi, J. C., Schar, J.-C., Waser, B., Wenger, S., Heppeler, A., Schmitt, J. S., and Macke, H. R. (2000) Affinity profiles for human somatostatin receptor subtypes SST1-SST5 of somatostatin radiotracers selected for scintigraphic and radiotherapeutic use. *Eur. J. Nucl. Med. Mol. Imaging* 27, 273–282.
- (2) Weckbecker, G., Lewis, I., Albert, R., Schmid, H. A., Hoyer, D., and Bruns, C. (2003) Opportunities in somatostatin research: biological, chemical and therapeutic aspects. *Nat. Rev. Drug Discovery* 2, 999–1017.
- (3) de Jong, M., Breeman, W. A. P., Bakker, W. H., Kooij, P. P. M., Bernard, B. F., Hofland, L. J., Visser, T. J., Srinivasan, A., Schmidt, M. A., Erion, J. L., Bugaj, J. E., Mäcke, H. R., and Krenning, E. P. (1998) Comparison of 111In-labeled Somatostatin Analogues for Tumor Scintigraphy and Radionuclide Therapy. *Cancer Res.* 58, 437–441.
- (4) Bakker, W. H., Krenning, E. P., Breeman, W. A., Kooij, P. P. M., Reubi, J.-C., Koper, J. W., de Jong, M., Laméris, J. S., Visser, T. J., and Lamberts, S. W. (1991) In Vivo Use of a Radioiodinated Somatostatin Analogue: Dynamics, Metabolism, and Binding to Somatostatin Receptor-Positive Tumors in Man. *J. Nucl. Med.* 32, 1184–1189.
- (5) Anderson, C. J., Pajean, T. S., Edwards, W. B., Sherman, E. L. C., Rogers, B. E., and Welch, M. J. (1995) In vitro and in vivo evaluation of copper-64-octreotide conjugates. *J. Nucl. Med.* 36, 2315–25.
- (6) de Jong, M., Breeman, W. A. P., Kwekkeboom, D. J., Valkema, R., and Krenning, E. P. (2009) Tumor Imaging and Therapy Using Radiolabeled Somatostatin Analogues. *Acc. Chem. Res.* 42, 873–880.
- (7) Lewis, J. S., Lewis, M. R., Srinivasan, A., Schmidt, M. A., Wang, J., and Anderson, C. J. (1999) Comparison of Four <sup>64</sup>Cu-Labeled Somatostatin Analogs in Vitro and in a Tumor-Bearing Rat Model: Evaluation of New Derivatives for Positron Emission Tomography Imaging and Targeted Radiotherapy. *J. Med. Chem.* 42, 1341–1347.
- (8) Sprague, J. E., Peng, Y., Sun, X., Weisman, G. R., Wong, E. H., Achilefu, S., and Anderson, C. J. (2004) Preparation and biological evaluation of copper-64-labeled Tyr<sup>3</sup>-octreotate using a cross-bridged macrocyclic chelator. *Clin. Cancer Res.* 10, 8674–8682.
- (9) Henze, M., Dimitrakopoulou-Strauss, A., Milker-Zabel, S., Schuhmacher, J., Strauss, L. G., Doll, J., Maecke, H. R., Eisenhut, M., Debus, J., and Haberkorn, U. (2005) Characterization of 68Ga-DOTA-D-Phe<sup>1</sup>-Tyr<sup>3</sup>-octreotide kinetics in patients with meningiomas. *J. Nucl. Med.* 46, 763–769.
- (10) Hicks, R. J. (2010) Use of molecular targeted agents for the diagnosis, staging and therapy of neuroendocrine malignancy. *Cancer Imaging* 10, 83–91.
- (11) Hofman, M. S., Kong, G., Neels, O. C., Eu, P., Hong, E., and Hicks, R. J. (2012) High management impact of Ga-68 DOTATATE (GaTate) PET/CT for imaging neuroendocrine and other somatostatin expressing tumours. *J. Med. Imaging Radiat. Oncol.* 56, 40–7.
- (12) Kong, G., Hofman, M. S., Murray, W. K., Wilson, S., Wood, P., Downie, P., Super, L., Hogg, A., Eu, P., and Hicks, R. J. (2016) Initial Experience With Gallium-68 DOTA-Octreotate PET/CT and Peptide Receptor Radionuclide Therapy for Pediatric Patients With Refractory Metastatic Neuroblastoma. *J. Pediatr. Hematol./Oncol.* 38, 87–96.

- (13) Veliky, I. (2015) Continued rapid growth in  $^{68}\text{Ga}$  applications: update 2013 to June 2014. *J. Labelled Compd. Radiopharm.* 58, 99–121.
- (14) McInnes, L. E., Rudd, S. E., and Donnelly, P. S. (2017) Copper, gallium and zirconium positron emission tomography imaging agents: The importance of metal ion speciation. *Coord. Chem. Rev.* 352, 499–516.
- (15) Laverman, P., McBride, W. J., Sharkey, R. M., Eek, A., Joosten, L., Oyen, W. J. G., Goldenberg, D. M., and Boerman, O. C. (2010) A Novel Facile Method of Labeling Octreotide with  $^{18}\text{F}$ -Fluorine. *J. Nucl. Med.* 51, 454–461.
- (16) Niedermoser, S., Wangler, B., Chin, J., Kostikov, A., Wangler, C., Bernard-Gauthier, V., Schirrmacher, R., Vogler, N., Soucy, J.-P., and McEwan Alexander, J. (2015) In Vivo Evaluation of  $^{18}\text{F}$ -SiFalin-Modified TATE: A Potential Challenge for  $^{68}\text{Ga}$ -DOTATATE, the Clinical Gold Standard for Somatostatin Receptor Imaging with PET. *J. Nucl. Med.* 56, 1100–5.
- (17) Lewis, J. S., Srinivasan, A., Schmidt, M. A., and Anderson, C. J. (1999) In vitro and in vivo evaluation of  $^{64}\text{Cu}$ -TETA-Tyr3-octreotate. A new somatostatin analog with improved target tissue uptake. *Nucl. Med. Biol.* 26, 267–273.
- (18) Paterson, B. M., Roselt, P., Denoyer, D., Cullinane, C., Binns, D., Noonan, W., Jeffery, C. M., Price, R. I., White, J. M., Hicks, R. J., and Donnelly, P. S. (2014) PET imaging of tumours with a  $^{64}\text{Cu}$  labeled macrobicyclic cage amine ligand tethered to Tyr<sup>3</sup>-octreotate. *Dalton Trans.* 43, 1386–1396.
- (19) Hicks, R. J., Jackson, P., Kong, G., Ware, R. E., Hofman, M. S., Pattison, D. A., Akhurst, T. A., Drummond, E., Roselt, P., Callahan, J., Price, R., Jeffery, C. M., Hong, E., Noonan, W., Herschtal, A., Hicks, L. J., Hedt, A., Harris, M., Paterson, B. M., and Donnelly, P. S. (2019)  $^{64}\text{Cu}$ -SARTATE PET Imaging of Patients with Neuroendocrine Tumors Demonstrates High Tumor Uptake and Retention, Potentially Allowing Prospective Dosimetry for Peptide Receptor Radionuclide Therapy. *J. Nucl. Med.* 60, 777–785.
- (20) Cullinane, C., Jeffery, C. M., Roselt, P. D., van Dam, E. M., Jackson, S., Kuan, K., Jackson, P., Binns, D., van Zuylen, J., Harris, M. J., Hicks, R. J., and Donnelly, P. S. (2020) Peptide receptor radionuclide therapy with  $^{67}\text{Cu}$ -CuSarTATE is highly efficacious against a somatostatin-positive neuroendocrine tumor model. *J. Nucl. Med.* 61, 1800–1806.
- (21) Huclier-Markai, S., Kerdjoudj, R., Alliot, C., Barbet, J., Bonraisin, A. C., Michel, N., and Haddad, F. (2014) Optimization of reaction conditions for the radiolabeling of DOTA and DOTA-peptide with (44m/44)Sc and experimental evidence of the feasibility of an in vivo PET generator. *Nucl. Med. Biol.* 41 (Suppl), e36–e43.
- (22) Walczak, R., Gaweda, W., Dudek, J., Choinski, J., and Bilewicz, A. (2019) Influence of metal ions on the  $^{44}\text{Sc}$ -labeling of DOTATATE. *J. Radioanal. Nucl. Chem.* 322, 249–254.
- (23) Baum, R. P., Singh, A., Benešová, M., Vermeulen, C., Gnesin, S., Köster, U., Johnston, K., Müller, D., Senfleben, S., Kulkarni, H. R., Türler, A., Schibli, R., Prior, J. O., van der Meulen, N. P., and Müller, C. (2017) Clinical evaluation of the radiolanthanide terbium-152: first-in-human PET/CT with  $^{152}\text{Tb}$ -DOTATOC. *Dalton Trans.* 46, 14638–14646.
- (24) Pauwels, E., Cleeren, F., Bormans, G., and Deroose, C. M. (2018) Somatostatin receptor PET ligands - the next generation for clinical practice. *Am. J. Nucl. Med. Mol. Imaging* 8, 311–331.
- (25) Deri, M. A., Zeglis, B. M., Francesconi, L. C., and Lewis, J. S. (2013) PET imaging with  $^{89}\text{Zr}$ : From radiochemistry to the clinic. *Nucl. Med. Biol.* 40, 3–14.
- (26) Boros, E., and Packard, A. B. (2019) Radioactive Transition Metals for Imaging and Therapy. *Chem. Rev.* 119, 870–901.
- (27) Noor, A., Van Zuylen, J. K., Rudd, S. E., Waldeck, K., Roselt, P. D., Haskali, M. B., Wheatcroft, M. P., Yan, E., Hicks, R. J., Cullinane, C., and Donnelly, P. S. (2020) Bivalent Inhibitors of Prostate-Specific Membrane Antigen Conjugated to Desferrioxamine B Squaramide Labeled with Zirconium-89 or Gallium-68 for Diagnostic Imaging of Prostate Cancer. *J. Med. Chem.* 63, 9258–9270.
- (28) Ward, M. C., Roberts, K. R., Babich, J. W., Bukhari, M. A., Coghlan, G., Westwood, J. H., McCreedy, V. R., and Ott, R. J. (1986) An antibody-desferrioxamine conjugate labeled with gallium-67. *Nucl. Med. Biol.* 13, 505–7.
- (29) Smith-Jones, P. M., Stolz, B., Bruns, C., Albert, R., Reist, H. W., Fridrich, R., and Maecke, H. R. (1994) gallium-67/gallium-68-[DFO]-octreotide—a potential radiopharmaceutical for PET imaging of somatostatin receptor-positive tumors: synthesis and radiolabeling in vitro and preliminary in vivo studies. *J. Nucl. Med.* 35, 317–25.
- (30) Wang, S., Lee, R. J., Mathias, C. J., Green, M. A., and Low, P. S. (1996) Synthesis, Purification, and Tumor Cell Uptake of  $^{67}\text{Ga}$ -Deferoxamine-Folate, a Potential Radiopharmaceutical for Tumor Imaging. *Bioconjugate Chem.* 7, 56–62.
- (31) Tsionou, M. I., Knapp, C. E., Foley, C. A., Munteanu, C. R., Cakebread, A., Imberti, C., Eykyn, T. R., Young, J. D., Paterson, B. M., Blower, P. J., and Ma, M. T. (2017) Comparison of macrocyclic and acyclic chelators for gallium-68 radiolabelling. *RSC Adv.* 7, 49586–49599.
- (32) Gourni, E., Del Pozzo, L., Bartholomä, M., Kiefer, Y., T. Meyer, P., Maecke, H. R., and Holland, J. P. (2017) Radiochemistry and Preclinical PET Imaging of  $^{68}\text{Ga}$ -Desferrioxamine Radiotracers Targeting Prostate-Specific Membrane Antigen. *Mol. Imaging* 16, 153601211773701.
- (33) Yokoyama, A., Ohmomo, Y., Horiuchi, K., Saji, H., Tanaka, H., Yamamoto, K., Ishii, Y., and Torizuka, K. (1982) Deferoxamine, a promising bifunctional chelating agent for labeling proteins with gallium: gallium-67 DF-HSA: concise communication. *J. Nucl. Med.* 23, 909–14.
- (34) Rudd, S. E., Roselt, P., Cullinane, C., Hicks, R. J., and Donnelly, P. S. (2016) A desferrioxamine B squaramide ester for the incorporation of zirconium-89 into antibodies. *Chem. Commun.* 52, 11889–11892.
- (35) Jacobsen, C. B., Raave, R., Pedersen, M. O., Adumeau, P., Moreau, M., Valverde, I. E., Bjoernsdottir, I., Kristensen, J. B., Grove, M. F., Raun, K., McGuire, J., Goncalves, V., Heskamp, S., Denat, F., and Gustafsson, M. (2020) Synthesis and evaluation of zirconium-89 labelled and long-lived GLP-1 receptor agonists for PET imaging. *Nucl. Med. Biol.* 82–83, 49–56.
- (36) Evers, A., Hancock, R. D., Martell, A. E., and Motekaitis, R. J. (1989) Metal ion recognition in ligands with negatively charged oxygen donor groups. Complexation of iron(III), gallium(III), indium(III), aluminum(III), and other highly charged metal ions. *Inorg. Chem.* 28, 2189–95.
- (37) Toporivska, Y., and Gumienna-Kontecka, E. (2019) The solution thermodynamic stability of desferrioxamine B (DFO) with Zr(IV). *J. Inorg. Biochem.* 198, 110753.
- (38) Holland, J. P. (2020) Predicting the Thermodynamic Stability of Zirconium Radiotracers. *Inorg. Chem.* 59, 2070–2082.
- (39) Poeppel, T. D., Binse, I., Petersenn, S., Lahner, H., Schott, M., Antoch, G., Brandau, W., Bockisch, A., and Boy, C. (2011)  $^{68}\text{Ga}$ -DOTATOC Versus  $^{68}\text{Ga}$ -DOTATATE PET/CT in Functional Imaging of Neuroendocrine Tumors. *J. Nucl. Med.* 52, 1864–1870.
- (40) Yang, J., Kan, Y., Ge, B. H., Yuan, L., Li, C., and Zhao, W. (2014) Diagnostic role of Gallium-68 DOTATOC and Gallium-68 DOTATATE PET in patients with neuroendocrine tumors: a meta-analysis. *Acta Radiol.* 55, 389–398.
- (41) Ma, M. T., Cullinane, C., Waldeck, K., Roselt, P., Hicks, R. J., and Blower, P. J. (2015) Rapid kit-based  $^{68}\text{Ga}$ -labelling and PET imaging with THP-Tyr3-octreotate: a preliminary comparison with DOTA-Tyr3-octreotate. *EJNMMI Res.* 5, 1–11.
- (42) Xia, Y., Zeng, C., Zhao, Y., Zhang, X., Li, Z., and Chen, Y. (2020) Comparative evaluation of  $^{68}\text{Ga}$ -labelled TATEs: the impact of chelators on imaging. *EJNMMI Res.* 10, 36.
- (43) Schottelius, M., Šimeček, J., Hoffmann, F., Willibald, M., Schwaiger, M., and Wester, H.-J. (2015) Twins in spirit - episode I: comparative preclinical evaluation of [ $^{68}\text{Ga}$ ]DOTATATE and [ $^{68}\text{Ga}$ ]HA-DOTATATE. *EJNMMI Res.* 5, 22.
- (44) Ishizaki, A., Mishiro, K., Shiba, K., Hanaoka, H., Kinuya, S., Odani, A., and Ogawa, K. (2019) Fundamental study of radiogallium-

labeled aspartic acid peptides introducing octreotate derivatives. *Ann. Nucl. Med.* 33, 244–251.

■ **NOTE ADDED AFTER ASAP PUBLICATION**

This paper was published on the Web on March 31, 2021. The Table of Contents/Abstract graphic was replaced, and the corrected version was reposted on April 8, 2021.